Evaluation of Asphalt Aging Using Multivariate Analysis Applied to Saturates, Aromatics, Resins, and Asphaltene Determinator Data

Lorris Bruneau, Séverine Tisse,* Laurent Michon,* and Pascal Cardinael

ACCESS | Metrics & More | Article Recommendations | Supporting Information

ABSTRACT: Asphalt is subjected to aging, leading to physical and chemical modifications reducing its performance. Recently, the Western Research Institute developed the SAR-AD method that allowed the separation of asphalt into eight fractions (saturates, aromatics 1, aromatics 2, aromatics 3, resins, asphaltenes 1, asphaltene 2, and asphaltenes 3). In this work, this analytical method was used to study asphalt aging processes in greater detail. Several asphalts of different origins and reconstituted blends were studied. These products were aged during several durations using a PAV (pressure aging vessel) between 0 and 48 h to collect information on the evolution of each SAR-AD fraction. Different evolutions were observed according to the initial asphalt composition and SAR-AD fraction studied. The saturated subfamily seemed to be slightly impacted by aging. The amount of three aromatic subfamilies decreased with a larger decrease of aromatics 3 than aromatics 2, itself larger than aromatics 1. The content of the resin subfamily increased after 48 h of PAV aging. The asphaltene 1 and asphaltene 2 subfamilies exhibited an increasing trend. Moreover, the quantity of asphaltenes 2 created seemed to correlate to the initial asphaltene content. The evolutions of the asphaltene 3 subfamily were not significant. However, a specific behavior was highlighted for the most asphaltenic sample. For this specific sample, the increase of resin content was weaker, the mass of asphaltenes 1 decreased, and the amount of asphaltenes 3 increased during aging. Given the large amount of data generated, an original approach was developed to statistically identify the most affected SAR-AD subfamily and determine correlations among them. Two PCAs (Principal Component Analysis) were conducted on asphalt SAR-AD data. This statistical analysis indicated two generic asphalt aging pathways. The first aging pathway could be the conversion of aromatics 2 into resins, with no evidence that resins could contribute to asphaltene creation. The second aging pathway showed the conversion of aromatics 3 directly into asphaltenes 2. These two aging pathways highlighted that the conversion of molecules in more polar ones during aging could skip SAR-AD subfamilies, meaning that asphaltenes could be created without involving resins.
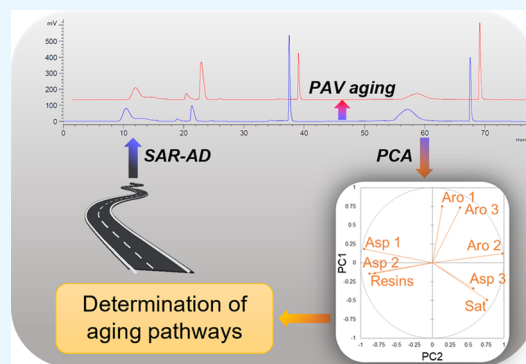
INTRODUCTION

Asphalt is a black viscoelastic material, often described as the least volatile fraction of petroleum. Due to its remarkable waterproofing and adhesive properties, it is successfully used in paving. Considering durability and sustainability, there has been much interest in asphalt aging. Many investigations have been performed to develop a better understanding of aging phenomena. Previous studies reported that this process generally impacts the physical performance of asphalt, as it results in asphalt hardening and eventually in excessive cracking.[1,2] However, the susceptibility to aging depends on the chemical composition of asphalt. The composition is directly linked to crude oils used in its production. The physical damage was proven to be linked to chemical composition evolution.[3,4]

A detailed understanding of chemical composition evolution during asphalt aging remains difficult due to the complexity of the asphalt matrix. To better understand aging, the pressure aging vessel[5] (PAV) is often used to age samples in the laboratory. It simulates asphalt oxidation after several years of

road service. For the chemical characterization of aged asphalt, several analytical techniques can be used. Elementary analysis[6] quantifies five principal atoms (CHNOS) of an asphalt sample and metal traces (vanadium, nickel, etc.) that can play a catalytic role during aging.[7,8] High-resolution mass spectrometry is useful in determining the detailed elementary composition and the molecular structure of compounds present in asphalt.[9,10] The most common spectroscopic technique used to assess aging impact is infrared spectroscopy. It monitors the evolution of specific functional groups during aging, specifically of oxygenated functional groups such as carbonyls, ketones, acids, or sulfoxides.[11−15] Two chromato-
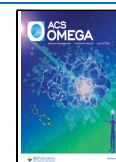
Table 1. Basic Physical Properties, Wax, and Asphaltene Contents of the Six Native Asphalt

| | | | asphalt | | | | | |
test	method	unit	A	B	C	G	S	F
penetration at 25 °C	EN 1426	mm/10	72	81	90	77	70	115
softening point	EN 1427	°C	47.4	46.4	46.0	48.0	48.0	46.2
kinematic viscosity at 100 °C	EN 12,596	mm²/s	2558	2413	2935	2056	4464	507
density	EN 15,326	g/cm³	1.020	1.018	1.036	1.027	1.037	0.990
wax content	PR T66-067	wt %	3.8	4.6	3.9	5.2	0.7	8.8
asphaltene content	NF T60-115	wt %	6.6	8.7	12.3	10.2	15.6	1.7

graphic techniques typically employed to study asphalt aging are gel permeation chromatography (GPC) and thin-layer chromatography combined with flame ionization detection (TLC-FID). GPC[16−18] tracks the increase in apparent molecular weight during aging due to the formation of aggregates. TLC-FID[17,19,20] was used to separate and quantify the relative amount of the four major molecular families. A similar quantification can also be obtained using the saturates, aromatics, resins, and asphaltenes (SARA) separation method developed by Corbett.[21] Recently, an original technology was developed by the Western Research Institute, SAR-AD.[22] It is a high-performance liquid chromatography method allowing the separation of asphalt into 8 molecular families instead of 4 using the common SARA separation. In fact, the SAR-AD allows the subdivision of each aromatic and asphaltene SARA fraction into 3 new subfamilies. As with the SARA method, a saturated subfamily is separated, mainly composed of long aliphatic chains.[23,24] Then, the aromatics 1, 2, and 3, mostly composed of aromatic rings, are recovered. The number of rings (between 1 and 5) increases from aromatics 1 to aromatics 3. Moreover, a low amount of heteroatoms can be measured in aromatics 3, leading to the highest polarity of the three aromatic subfamilies. The resin subfamily, also recovered with the SARA separation, is more polar than the aromatic subfamilies. The resins have a chemical structure close to that of aromatics 3, but they contain a larger amount of heteroatoms. The last three subfamilies separated by the SAR-AD are asphaltenes 1, 2, and 3. Typically, they are highly polycondensed molecules and contain a large amount of heteroatoms (nitrogen, oxygen, and sulfur).

All of these analytical techniques previously presented allow the evaluation of the impact of aging on asphalt chemistry and have been used in many studies. Mirwald[25,26] studied the aging impact on the SARA fraction and observed that the aging process chemically results in an increase in average polarity. The polarity increase varies with the aging method used and asphalt origin. Generally, the content of saturates during aging exhibited a very slight decrease, while the aromatic fraction content showed a drastic decrease. The amount of asphaltenes increased due to the oxidation of less polar molecules. The last SARA fraction of asphalt is the resins, which have a polarity between that of aromatics and asphaltenes. Usually, the amount of resin increases during aging. Nevertheless, Hung and Fini[27] pointed out that resins could also exhibit a different evolution throughout the aging period. In their work, the amount of resin initially decreased during aging, followed by an increase at a later stage. The use of the SAR-AD can permit investigation into the evolution of the three aromatic and asphaltene subfamilies, potentially providing additional insights into chemical changes of saturates, aromatics, resins, and asphaltene content compared to using the SARA separation methodology. As a consequence of this, a finer understanding

of aging impact can be developed, allowing the identification of the transfer of molecules from one subfamily to another.

Multivariate analyses, such as principal component analysis (PCA), have recently been used in asphalt fields. For instance, PCA was recently used to identify the source of asphalt from attenuated total reflectance-Fourier transform infrared (ATR-FTIR) spectra.[28,29] PCA can also be used to study asphalt aging. For instance, Margaritis et al.[30] used PCA on chemical and rheological data of reclaimed asphalts to evaluate their aging states. Lacroix-Andrivet et al.[9] applied PCA to high-resolution mass spectrometry data to classify asphalt according to its PAV aging state and origin. PCA appears to be an interesting statistical tool to provide a better understanding of aging impacts on the evolutions of SAR-AD subfamilies.

In this study, an original approach was proposed to investigate molecular conversion from one SAR-AD subfamily to another subfamily during PAV aging.

Six asphalts of different origins were selected to cover a large range of initial asphaltene contents from 1.7 to 15.6 wt %. The maltenic fraction (saturate, aromatic, and resin fractions) of three of them was separated and collected by precipitation in n-heptane. Furthermore, five asphalt blends were prepared by mixing one asphalt with asphaltenes or maltenes from n-heptane separated fractions. This sample panel allowed us to compare the aging impact on both asphalt samples coming from different origins and those containing the same initial asphaltene content. Asphalts, maltenes, and asphalt blends were aged with the PAV for 8, 16, 24, and 48 h. Neat and aged samples were analyzed with SAR-AD to quantify the 8 molecular subfamilies. PCA was applied to the collected dataset to highlight aging pathways.

■ MATERIALS AND METHODS

Studied Asphalts. Six asphalts referenced A, B, C, F, G, and S were selected for this study. These asphalts were produced by the direct distillation of petroleum crudes. According to the EN 12591 standard,[31] all of them are classified as asphalt 70/100, except for asphalt F, which is an asphalt 100/150 (based on their range of penetration at 25 °C). Their conventional properties measured with normalized methods are provided in Table 1. For the study, the codification of asphalt (Table 2) is composed of two letters: first, there is a B (for bitumen), followed by a second letter representing the origin (A, B, C, G, S, or F).

Asphalt Separation Protocol. The studied asphalts F, G, and S were separated into asphaltenes and maltenes obtained by applying a modified version of the ASTM D4124 protocol.[32] Asphaltenes are defined as asphalt molecules insoluble in an n-alkane when the soluble fraction constitutes the maltenes. For this separation, the solvent and filter chosen were those used in the ASTM D4124 protocol.[32] The authors want to underline that the choice of n-alkane solvent (chain

Table 2. Codification and Formula of All Samples

code	asphalt origin	maltene origin	asphaltene origin	asphaltene content (wt %)
BA	A			6.6
BB	B			8.7
BC	C			12.3
BF	F			1.7
BG	G			10.2
BS	S			15.6
MF		F		≈1.0
MG		G		≈1.0
MS		S		≈1.0
BGAG	G		G	15.5
BGAS	G		S	15.5
BSMS	S	S		10.0
BFAS	F		S	10.0
BFAG	F		G	10.0

length) and the filter porosity have a significant impact on the molecular composition of asphaltenes (dimerization and agglomeration of asphaltene compounds) recovered. Moreover, this separation is solubility-based; agglomerates of asphaltene molecules after separation, which have lost hindering forces, will have different solubilities in the same solvent. The experimental protocol consisted of dissolving 10 g of asphalt in 1 L of *n*-heptane (purity ≥99.0%) while refluxing solvent for 2 h. The samples of solution phase maltenes and precipitated asphaltenes were cooled down at room temperature over 2 h. This solution was filtered through a 10 μm PTFE filter. Asphaltenes were filtered and cleaned with 50 mL of fresh *n*-heptane several times. The maltenes were recovered after evaporation of the *n*-heptane. Maltenes are labeled with two letters (Table 2): the first letter is M for maltenes, and the second letter represents F, G, or S, which represents the original asphalt from which the sample was prepared.

Asphalt Blend Preparation. In addition to the six asphalts mentioned above, five new asphalts were prepared to assess the effects of a change in the asphaltene content of asphalts F, G, and S. To complete this objective, the initial ratio between the asphaltene and maltene content of those three asphalts was (F, G, and S) modified by adding asphaltenes or maltenes obtained according to the protocol previously described. The method to prepare blends by either adding asphaltenes (powder) or maltenes (semi-pasty liquid) to the original asphalts was different due to the physical nature of both products and is described below.

The addition of asphaltenes to asphalt required dissolving both components in a solvent to ensure good mixing of the powder. The solvent was subsequently removed to obtain the new asphalt blend. Both samples were accurately weighed to achieve the desired final asphaltene content, diluted together in dichloromethane (10 times the sample volume, purity ≥99%), and manually stirred for 5 min. Dichloromethane was then removed by evaporation at ambient temperature for one night under a laboratory hood, followed by 45 min in a vacuum oven at 150 °C and 350 mbar. To ensure the complete evaporation of solvent at the end of the process, an ATR-FTIR (attenuated total reflectance-Fourier transform infrared) analysis was performed by checking for the presence of dichloromethane bands. If needed, the evaporation step in the vacuum oven was repeated until the infrared dichloromethane bands totally disappeared from the spectrum.

The addition of maltenes to asphalt is more straightforward than blending with asphaltenes. Maltenes and asphalt were heated at 100 and 160 °C, respectively, before adding a precise quantity of maltene to a defined quantity of asphalt to reach the desired final concentration of asphaltenes. The blends were manually mixed for 2 min to achieve a homogeneous blend.

Approximately 25 g of asphalt-maltene/asphaltene blends were prepared, which is a consistent size of the sample required for analysis by the methods used in this study.

Regarding the addition strategy, asphaltenes from asphalts G and S were added to asphalts G and F to reach 15.6 and 10 wt % of asphaltenes, respectively, which corresponds to the initial asphaltene content of asphalts S and G (Table 2). Along the same approach, maltenes S were added to asphalt S to target a final content in asphaltene (10 wt %) corresponding to asphalt G (Table 2). The first objective of this blend preparation was to compare several asphalt samples coming from the same origin, so presenting the same molecular composition but in different proportions (for example, asphalt S, blend S, and maltene S). The second one was to compare asphalt with the same content of asphaltenes but from different origins (molecular composition). These differences in the SAR-AD subfamily amount before PAV aging for samples coming from the same origin could allow us to better understand the subfamily role and their correlations during the aging process.

The addition of asphaltenes or maltenes changed the proportion of the different molecular fractions. According to Mousavi et al.,[33,34] these changes in chemical composition could impact the colloidal stability as the addition of maltene to asphalt can work as a modifier affecting asphaltene stacking. For example, the resin molecules clearly stabilize the asphaltene dimers.

Blends are summarized in Table 2, which also provides the products labeled as follows: the first letter (B) means bitumen (asphalt), the second letter (F, G, or S) indicates the origin of the asphalt that was modified, the third letter (A or M) indicates if the modification was made with asphaltenes (A) or maltenes (M), and the last letter (F, G or S) informs on the origin of used asphaltenes or maltenes. For example, asphalt BGAS means that asphalt G was modified with asphaltenes obtained from asphalt S.

Asphalt Aging Protocol. To assess how asphalt properties change during aging, the PAV (pressure aging vessel) long-term aging test was applied to studied asphalts. The PAV test attempts to simulate asphalt aging that occurred after several years of pavement service life. Typically, PAV test operating conditions for temperature and pressure fixed at 100 °C and 21 bar, respectively, were used (following EN 14,769[5]). In this study, multiple aging durations were chosen to determine how asphalt composition changes with the aging time (8, 16, 24, and 48 h). In addition, sampling cups were selected to receive 3 g of asphalt instead of 50 g (for EN 14,769)—corresponding to a diameter of 44 mm instead of 140 mm to accommodate the limited quantity of material available for testing. Using 3 g of asphalt in this specific sampling cup results in a thinner sample than the sample used with the standard method (2.0 mm instead of 3.3 mm). One asphalt was aged using these two sampling cups with different masses, 3 g in the smallest cup and 50 g in the biggest cup, respectively. A slight increase of the carbonyl index from 0131 to 0156 and the sulfoxide index from 0607 to 0716 measured by FTIR analysis[35] was observed when using the smallest sampling cup.
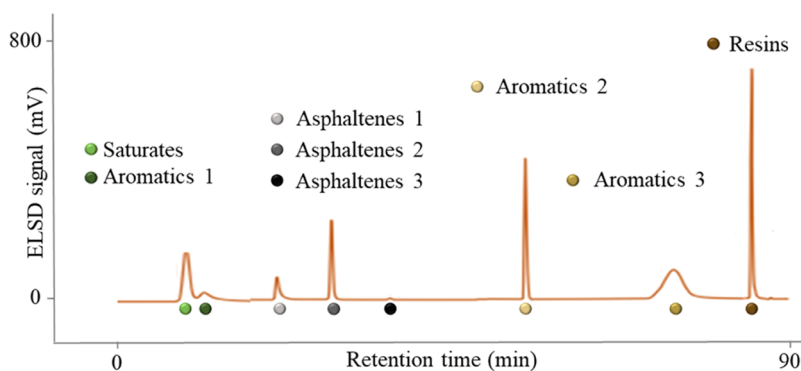
Figure 1. Example of the asphalt SAR-AD chromatogram using operating conditions previously described by the WRI, injection volume = 20 μL, asphalt at 5 wt % in chlorobenzene.
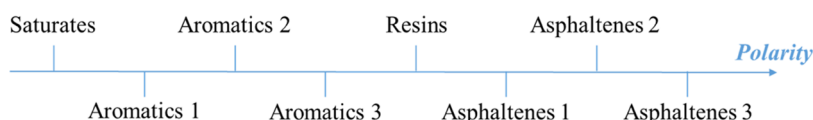

Figure 2. Polarity scale of the 8 SAR-AD subfamilies.

Oxidation time is denoted in the sample labels. The number in the sample label represents the oxidation time (0, 8, 16, 24, or 48) in PAV (in hours). For example, sample BF8 means that the asphalt F is oxidized 8 h in PAV.

SAR-AD Separation Protocol. SAR-AD (saturates, aromatics, resins, and asphaltene determinator)[22] is an HPLC (high-performance liquid chromatography) methodology developed and patented by the WRI (Western Research Institute) to separate the molecular continuum of asphalt into 8 subfamilies (saturates, aromatics 1, aromatics 2, aromatics 3, resins, asphaltenes 1, asphaltenes 2, and asphaltenes 3).

This equipment consists of a set of four columns packed with four different stationary phases. Asphalt molecules were separated based on their relative polarity on those columns using four different mobile phases. Molecules were detected after separation using an evaporative light scattering detector (ELSD). The SAR-AD operating conditions were the same as previously described[22] by the WRI. The tested samples were dissolved in chlorobenzene (HPLC quality) at 10% by mass. Figure 1 provides an example of a chromatogram obtained after asphalt separation on SAR-AD equipment. Finally, an external calibration was used to calculate the mass of each family.

ELSD was chosen for SAR-AD detection due to its capability to detect all chemical compounds from asphalt. However, ELSD response coefficients depend on mobile phase composition, the nature of analyzed molecules, and operating conditions.[36] Moreover, the ELSD response is nonlinear as a function of the injected sample mass. As a consequence of these ELSD response variables, an external calibration for each SAR-AD subfamily was used to estimate their content by mass. Preparative separation of asphalt was performed several times to collect sufficient quantities of all eight SAR-AD subfamilies to use as calibration standards. For each of the eight SAR-AD subfamilies, a calibration curve was established using these collected standards. The calibration methodology was critical to accurately quantify how PAV aging changed molecular distributions across the eight SAR-AD subfamilies.

Multivariate Analysis. The six asphalts A, B, C, F, G, and S were aged according to the protocol described in section

Asphalt Aging Protocol. Neat and aged asphalts were analyzed by SAR-AD according to the protocol described in the section SAR-AD separation protocol. Ultimately, 240 data points were generated (6 asphalts, 5 aging durations, on which the 8 SAR-AD subfamilies were collected).

To evaluate the collected data, a multivariate analysis approach was applied using XLSTAT statistical and data analysis solution (Addinsoft software version 2022.1.2). As part of the available multivariate methods, principal component analysis (PCA), hierarchical cluster analysis (HCA), discriminant factor analysis (DFA), and partial least squares (PLS) were explored. The data were normalized before starting the multivariate analysis.

Principal component analysis (PCA) was chosen for the study; it is a descriptive nonsupervised method whose purpose is to present the maximum amount of information contained in a dataset consisting of p quantitative variables for n individuals. PCA permits the dimensionality of the original dataset to be reduced by calculating a set of new variables named principal components (PCs). This data mining technique can help researchers shed light on similarities between samples and/or a relationship between variables.
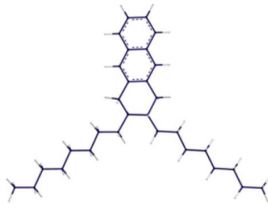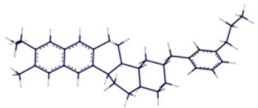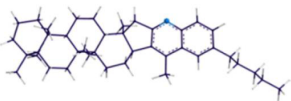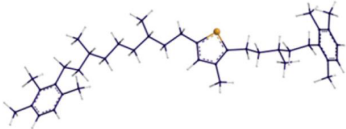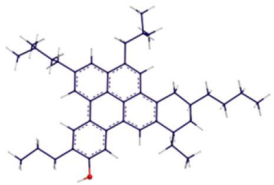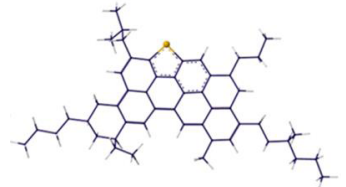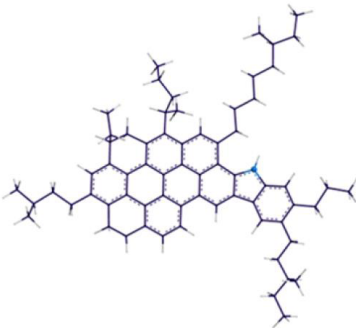
SAR-AD data determined on asphalt-maltene/asphaltene blends (described in Table 2) and maltenes obtained by separation of asphalts F, G, and S, as well as FTIR data on all products, are considered as supporting data used in a second step for the multivariate analysis.

■ RESULTS

In this paper, asphalts, maltenes, and asphalt blends were aged during several PAV durations to monitor the evolution of chemical composition. For the specific case of asphalt blend, it is important to keep in mind that the asphaltene/maltene blending after separation could have a colloidal structure different from nonmodified asphalt. For example, as described by Pahlavan et al.,[37] the addition of conjugated aromatics could promote the deagglomeration of polyaromatic aggregates, such as self-assembled stacks of oxidized asphaltenes.

Chemistry of the SAR-AD Families and Global Aging Impact. In this section, an explanation is provided to describe

Table 3. Association of a Model Molecule Proposed by Mousavi et al.[38] for each SAR-AD Subfamily

SAR-AD subfamily	Model molecule [38]	Polarizability (Bohr) [38]
Saturates		353.52
Aromatics 1		350.91
Aromatics 2		404.06
Aromatics 3		460.36
Resins		472.08
Asphaltenes 1		527.01
Asphaltenes 2		675.98
Asphaltenes 3		875.29

how each SAR-AD subfamily is affected by PAV aging. This would also be related to their molecular structure and polarity.

Knowing that asphalt aging leads to an increase in the polarity of the molecule, it is important to be able to classify the 8 SAR-

AD subfamilies according to their polarity. Figure 2 presents the polarity scale of the 8 SAR-AD subfamilies according to their chromatographic elution. Moreover, the SAR-AD subfamily quantities on the original samples are provided in Table S1.

Based on the 10 asphalt molecules and their polarizability calculated with density functional theory (DFT),[38] association between the SAR-AD subfamily and model molecules is proposed in Table 3.

During PAV aging, SAR-AD subfamily contents can increase or decrease for the studied products. To follow their evolution during the aging process, results were provided in percentages of change and not in absolute values. This allowed the identification of general trends and identification of specific behaviors.

Evolution of the Saturate Subfamily during PAV Aging. The quantity of saturates, the less polar molecules, exhibited only small variations during aging (a slight decrease of a few percentages was observed in some samples). This observation was not unexpected, considering that their chemistry is mostly composed of long aliphatic chains.[39,40] As a consequence of this, they were less sensitive to oxidation, which is consistent with previous works studying the impact of aging on saturated fraction.[25,26]

Evolution of the Aromatic 1 Subfamily during PAV Aging. Aromatics 1 are the least polar molecules of the three SAR-AD aromatic subfamilies. As per Adams et al.[39] work, aromatics 1 typically contain one aromatic ring. For this aromatic subfamily, a decrease from 0.5 to 10.5% of their content was observed after 48 h of PAV aging (Figure 3). Sample BF was
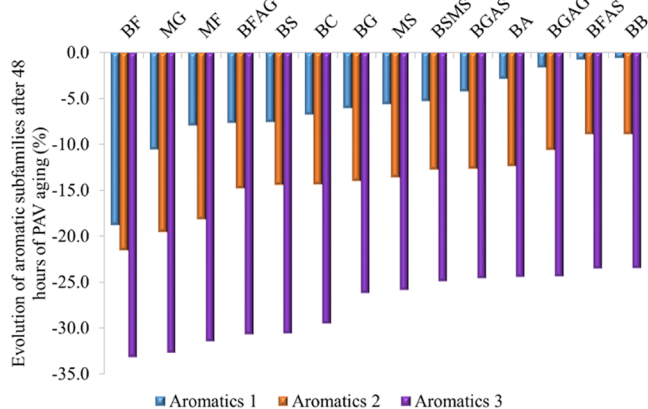

Figure 3. Evolution (in %) of the three SAR-AD aromatic subfamilies after 48 hours of PAV aging for all studied samples.

the exception, which shows an aromatics 1 decrease of 19.0%. In general, the aromatic 1 subfamily was the least impacted by oxidation when compared to changes observed for aromatic 2 and 3 SAR-AD subfamilies (described later in the document) (Figure 3) consistent with the polarity/reactivity of these SAR-AD subfamilies.

Evolution of the Aromatic 2 Subfamily during PAV Aging. This subfamily is slightly more polar than aromatic 1 due to a greater number of aromatic rings, typically two or three fused together. For all samples, the decrease in aromatics 2 was greater than that for aromatics 1, from 8.9 to 21.5% after 48 h of PAV aging (Figure 3). Aromatics 2 appeared to be more sensitive to oxidation. Here, all data were regularly spread between the two extreme values reported above for aromatics

2. BF exhibited the highest percentage from the series after 48 h of PAV aging, but the difference in results with other asphalts was not as significant as for aromatics 1.

Evolution of the Aromatic 3 Subfamily during PAV Aging. The aromatic 3 subfamily is characterized by the highest polarity of the three aromatic subfamilies, with molecules having four to five rings and a small amount of heteroatoms. This subfamily is also the most abundant SAR-AD fraction in neat asphalts used in this study. After 48 h of PAV aging, this subfamily presented a decrease in aromatics 3 ranging from 23.5 to 33.2% (Figure 3). As with the aromatic 2 subfamily, the same observations were made that asphalt BF demonstrated the largest absolute change in aromatics 3.

From the above results, it was observed that the higher the polarity of the aromatic subfamilies, the greater the oxidation effect. This behavior was consistent with what is typically observed in chemistry when the level of aromatic ring polycondensation increases. To illustrate this trend, Figure 3 presents the decrease in the three SAR-AD aromatic subfamilies after 48 h of PAV aging for all studied samples.

Evolution of the Resin Subfamily during PAV Aging. According to Figure 2, the SAR-AD resin subfamily is more polar than the saturated and aromatic fractions. Their chemical structure is not that different from that of aromatics 3 regarding the number of aromatic fused rings, but they are characterized by more heteroatoms and polar functional groups, such as alcohols.[39] This subfamily is very sensitive to oxidation processes. For the studied materials, their content in the resin subfamily after 48 h of PAV aging increased from 4.5 to 65.5%, depending on the tested asphalt. Within the resin subfamily, BF did not present a behavior significantly different from the other studied asphalts, which was different from the changes with the aromatic subfamilies as previously described. In this study, regardless of the base asphalt tested, the saturated and aromatic subfamilies were characterized by a regular and continuous evolution of their content during the different PAV duration applied (8, 16, 24, and 48 h) (Table S1). This trend was also true for the resin subfamily except for asphalts BS, MS, and BSMS. In these asphalts, 8 h of PAV aging resulted in an increase in the resin content, followed by a regular decrease or a constant evolution up to 48 h of aging. The 4.5% reported above corresponded to the results obtained with BS. At this stage, no specific explanation could be provided, except that BS has the highest asphaltene content (15.6 wt %) of the asphalts studied.

From the above results, a significant increase in the resin subfamily content was observed after 48 h of PAV aging, except for products from the asphalt S origin (Figure 4).

Evolution of the Asphaltene 1 Subfamily during PAV Aging. Prior to describing observations made for the asphaltene 1 subfamily, it is important to provide some information about the asphaltenes in general. The chemistry of the asphaltenes was studied by D'melo et al.[41−44] They showed that nitrogen, oxygen, and sulfur are largely present in those molecules with a H/C ratio, indicating a higher level of polycondensation than reported for other subfamilies. Consequently, asphaltenes 1, 2, and 3 are the most polar subfamilies in asphalt.

As SAR-AD allows the separation of asphaltenes into three subfamilies, asphaltene 1 is the least polar fraction among the asphaltenes (Figure 2). During the 48 h of PAV aging, there was an increase in asphaltene 1 content in all studied samples except for BS and BSMS (Figure 5). In general, the increase
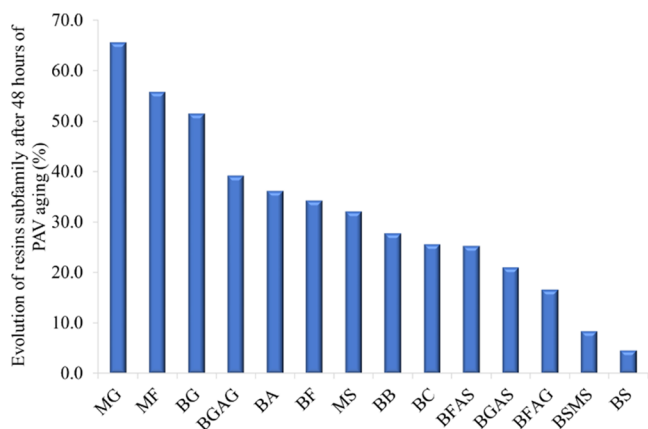
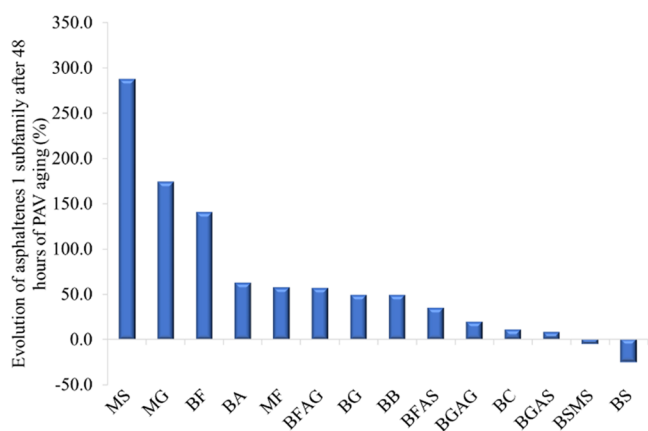**Figure 4.** Evolution (in %) of the SAR-AD resin subfamily after 48 h of PAV aging for all studied samples.

Figure 5. Evolution (in %) of the SAR-AD asphaltene 1 subfamily after 48 h of PAV aging for all studied samples.
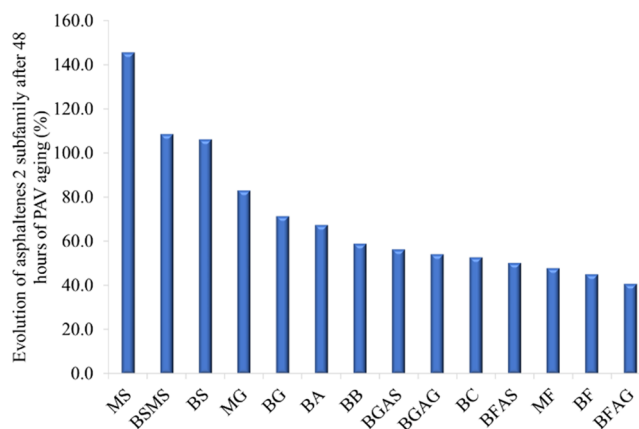

Figure 6. Evolution (in %) of the SAR-AD asphaltene 2 subfamily after 48 h of PAV aging for all studied samples.

asphaltene content was consistent for all asphalts. This observation is illustrated in Figure 7.
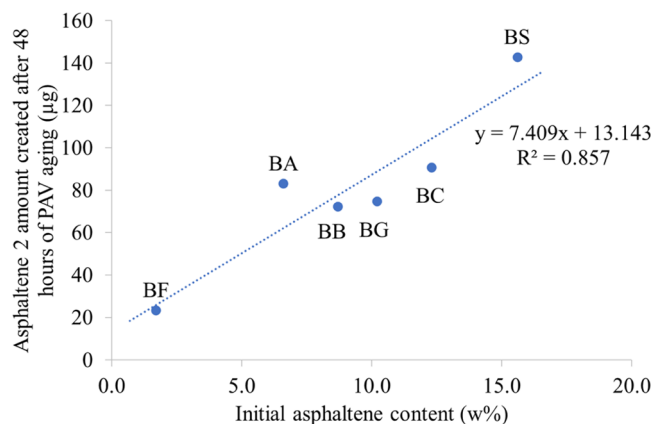

Figure 7. Relationship between the amounts of SAR-AD asphaltene 2 created after 48 h of PAV aging and initial total asphaltene contents (NF T60-115) for the 6 studied asphalts.

ranged from 8.0 to 287.7%. Again, products from asphalt S showed a different behavior with a decrease in asphaltenes 1 after 48 h of PAV aging. As observed for the Asphalt S resin subfamily, until 8 h of PAV aging, an increase in asphaltene 1 content was observed, followed by a regular decrease up to 48 h of aging.

Evolution of the Asphaltene 2 Subfamily during PAV Aging. The asphaltene 2 subfamily is the most abundant among the asphaltenes. According to D'melo et al.,[41] asphaltene 2 contained more oxygen, nitrogen, and sulfur, and the H/C ratio was lower than that of asphaltene 1. For all of the samples, the percentage of this SAR-AD subfamily increased during all 48 h of PAV aging, ranging from 40.7 to 145.5% after 48 h of PAV. These results are presented in Figure 6.

Asphaltenes 2 increased in all samples over 48 h of PAV aging, but the absolute quantity of asphaltenes 2 created was different for each sample. The creation of asphaltene 2 molecules appeared to be partly linked to the initial total asphaltene content. Considering the 6 asphalts, the largest amount of asphaltene 2 molecules created during the 48 h of PAV aging was in BS (143 μg). It was the most asphaltenic product (15.6 wt %), whereas the lowest asphaltene 2 quantity created was in BF (23 μg), an asphalt with only 1.7 wt % of asphaltenes before aging. The relationship between the creation of asphaltenes 2 during aging and the original total

Evolution of the Asphaltene 3 Subfamily during PAV Aging. Among the three asphaltene subfamilies, asphaltenes 3 is the most polar fraction; they are composed of large molecules with a lot of heteroatoms and aromatic fused rings. Their behaviors during PAV aging were different from asphaltenes 1 and 2. In most of the studied samples, the amount of asphaltene 3 exhibited an evolution of around ± 20% after 48 h of PAV aging. The negative evolution observed for BFAG, MF, BG, and BF corresponded to a decrease of their asphaltene 3 content. However, meaningful interpretation of observed changes with increased aging for most samples is confounded by the small quantities and small changes of asphaltene 3 (only a few μg), which means changes observed are largely within experimental variability. The exceptions to this comment were samples BS, BSMS, and MS, which respectively presented an increase of asphaltenes 3 of 66.6, 89.1, and 136.8% over the 48 h of aging. The results are summarized in Figure 8.

The study of asphaltene 3 evolution in asphalts G and F doped with asphaltene S (BFAS and BGAS) allowed us to potentially determine the source of this specific behavior seen in asphalt S. BFAS and BGAS exhibited a very small increase in their asphaltene 3 amount during PAV aging, despite the
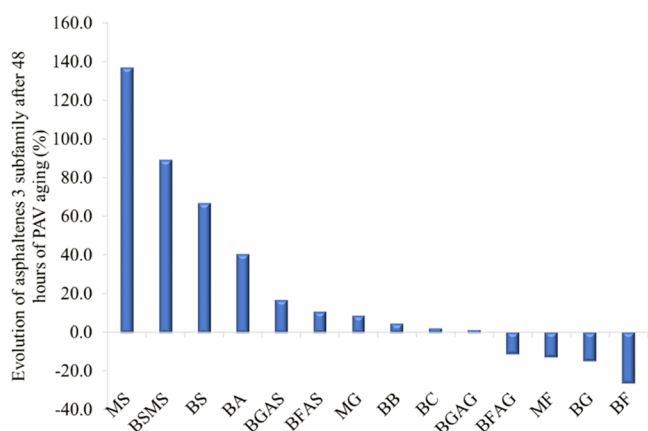
Figure 8. Evolution (in %) of the SAR-AD asphaltene 3 subfamily after 48 h of PAV aging for all studied samples.

presence of asphaltenes S. The combination of these previous observations suggested that the creation of asphaltenes 3 during PAV aging could be due to the maltenic fraction of asphalt S.

To summarize, this study highlighted the global evolution of each SAR-AD subfamily during aging for all studied asphalts. In general, saturates, aromatics 1, 2, and 3, and asphaltenes 2 exhibited similar trends for all studied asphalts. The quantity of saturates remained almost constant, the quantity of aromatics 1, 2, and 3 decreased, and the asphaltene 2 content increased during the aging time. However, this work also allowed us to note the particular behaviors of resins and asphaltenes 1 and 3 in asphalt S during PAV aging. A reduction in the resin and asphaltene 1 contents after 8 hours of PAV and an increase in the asphaltene 3 amount over 48 hours of aging were observed.

Following these specific observations for asphalt S, maltenes, and asphalt blends were used to suggest several explanations:

- The regular decrease/constant evolution of resin content taking place after 8 h of PAV aging was also observed in MS and BSMS but not in the other maltenes and asphalt blends, even BFAS, which was spiked with asphaltene S. The origin of this particular phenomenon could be related to the maltenic fraction of asphalt S.
- The decrease of asphaltene 1 content observed in asphalt S after 8 h of PAV aging also appeared in BSMS but not in MS. This observation suggested that this specific evolution took place in samples containing both maltenes S and asphaltenes S.
- The increase of asphaltene 3 content noticed in asphalt S during PAV aging was also observed in BSMS and MS but not in all other maltenes and blends, even if they were spiked with asphaltenes S. As a consequence of these observations, it could be suggested that the origin of asphaltenes 3 increases was due to the maltenic fraction of S.

Moreover, thanks to the study of products coming from the same origin asphalt but containing different total asphaltene contents, for example, MS, BSMS, and BS, the relationship between the amount of asphaltenes 2 creation and the initial total asphaltene content was confirmed.

The findings described above were made by observing how the amounts of different SAR-AD subfamilies vary during PAV aging. At this stage, this provided a broad picture of how the SAR-AD subfamilies changed but did not indicate how

molecules interacted together and what the preferred aging pathways were. To address this point, a principal component analysis was conducted, and the results are described in the next section.

PCA on SAR-AD Data. The SAR-AD analysis of the six neat and corresponding aged asphalts provided a database of 30 individual samples, and for each asphalt, the 8 molecular subfamilies were quantified, allowing the generation of 240 individual data points. Quantities of the 8 molecular subfamilies were considered variables. The results obtained with the 6 neat and aged asphalts were the only data used to generate the first PCA. Asphalt blends were not used to calculate the PCA considering that the colloidal structure could be affected by the blending step. The first step of the PCA study was to determine the optimum number of principal components and to understand their significance. The second step of the PCA study consisted of classifying asphalts and defining preferred aging pathways (transformation of molecules from one SAR-AD subfamily to another during aging).

The PCA was performed on a limited database. The findings made from this statistical analysis are correct for the studied samples. With a larger panel of asphalts, findings could be adjusted.

The first step of a PCA is to choose the number of principal components to be considered for the study without losing too much information. The scree plot in Figure 9 shows the
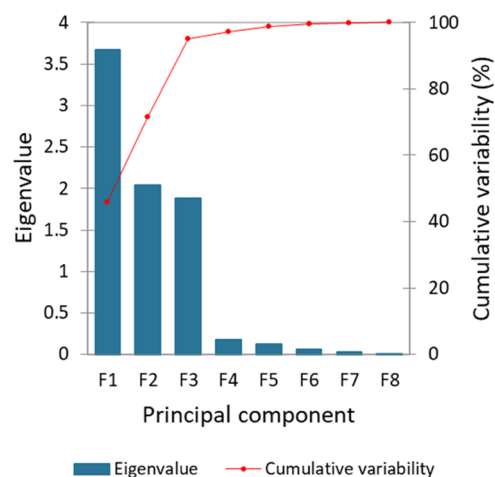

Figure 9. PCA scree plot obtained with the SAR-AD database of 6 asphalts. The Eigenvalue (blue histogram) is the variance obtained on each principal component. The cumulative variability (red line) represents the cumulative percentage of variance explained by the principal components.

cumulative variability explained by PCA according to the number of principal components (PCs) used. The first three PCs, called F1, F2, and F3, explained 45.8, 25.5, and 23.6%, respectively, to reach a cumulative variability of the data of 94.9%, which is an excellent result. The chosen model for the PCA allows working with 3 new variables instead of 8 SAR-AD variables without giving up more than 5% of the information.

The second step of the PCA analysis was to attempt to determine the parameter represented by each PC. The three circles of correlation in Figure 10 were constructed with the 3 PCs chosen for the study and the 8 variables corresponding to the 8 SAR-AD subfamilies. In addition, oxidation time was added to the PCA as an additional variable to improve the
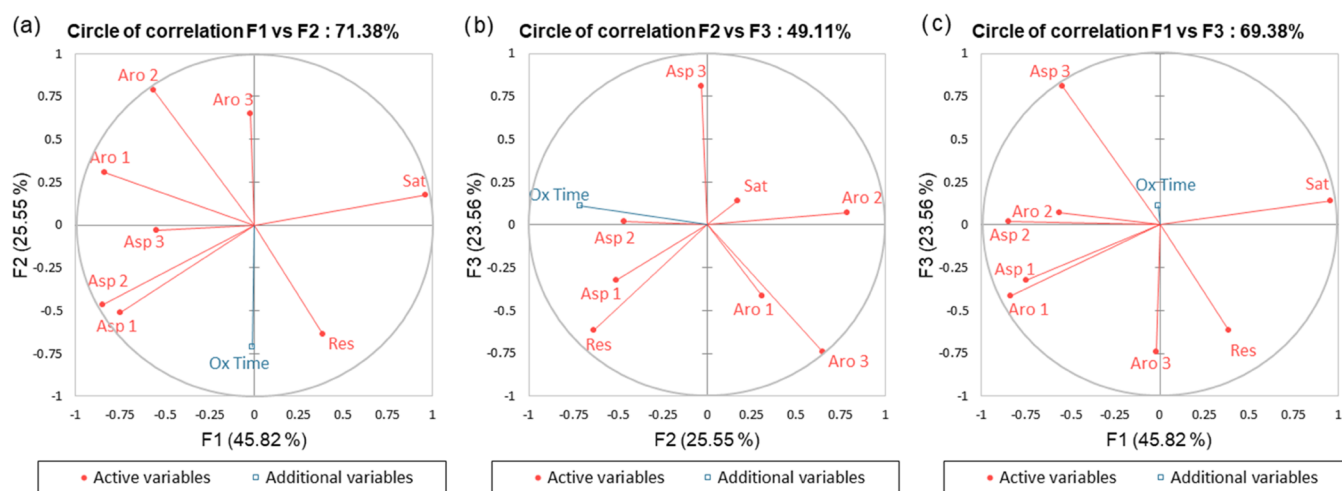
Figure 10. Circles of correlation calculated with the 6 asphalts (a) F1 vs F2: 71.38% of variability explained, (b) F2 vs F3: 49.11% of variability explained, (c) F1 vs F3: 69.38% of variability explained.

interpretation of PC significance. The interpretation of the different correlations between variables and principal components was facilitated by the correlation values in Table 4. In

Table 4. Correlation between Studied Variables and Principal Components[a]

variables	F1	F2	F3
saturates	**0.959**	0.172	0.143
aro 1	**−0.837**	0.306	−0.414
aro 2	−0.563	**0.788**	0.073
aro 3	−0.021	**0.647**	**−0.739**
resins	0.384	**−0.637**	−0.617
asp 1	**−0.750**	−0.509	−0.321
asp 2	**−0.847**	−0.464	0.019
asp 3	−0.549	−0.032	**0.811**
oxidation time in PAV	−0.009	**−0.713**	0.110

[a]Bold values are values greater than at |0.620| and considered significant.

this table, all values above 0.620 and below −0.620 (value calculated from Anderson formula[45]) have been bolded because a high value indicated a significant correlation between the variable and the principal component.

The results in Table 4 showed that the first principal component, F1, was highly correlated with the saturated variable and anticorrelated with asphaltenes 1 and 2. F2 was correlated with aromatics 2, aromatics 3, and the resins but was anticorrelated with oxidation time; as a result, F2 translated the PAV aging effect on the asphalt chemical composition well. The last principal component, F3, was highly correlated with asphaltenes 3 and anticorrelated with the aromatic 3 variable.

The determination of the correlation between variables in Figure 10 was conducted upon the study of a vector's size and direction. A variable is well represented in a circle of correlation if the vector is close to the ring. Moreover, to determine a correlation between two variables, it is necessary to study angles formed between vectors. If two vectors are superimposed (angle ≈ 0°), they are correlated, and if they form an angle of ≈ 180°, they are anticorrelated. However, if an angle of ≈ 90° is formed, there is no correlation between the variables. Plan F1—F2, represented in Figure 10a, was the most informative, with 71.4% of the variability explained. In

this plan, 6 active variables were well represented (saturates, aromatics 1 and 2, resins, and asphaltenes 1 and 2) due to the significant length of their vectors. The second circle of correlation presented in Figure 10b was made with the principal components F2 and F3. It only revealed 49.1% of the variability. In this figure, only 4 active variables had a vector near the circle (aromatics 2 and 3, resins, and asphaltenes 3). The F1—F3 plan (Figure 10c) was not linked to the oxidation time because this variable was only correlated with F2, which was perpendicular to this plan by definition. Consequently, correlations between variables were not studied in detail in this plan because they were not linked to aging phenomena. From the 2 circles of correlations taking into account the oxidation time (Figures 10a,b), all observed correlations between the different variables are summarized in Table 5.

Table 5. Summary of Correlations between Variables Deduced from the Two Circles of Correlation Considering Oxidation Time

plan	anticorrelation	correlation	no correlation
F1—F2	aro 2—resins	asp 1—asp 2	aro 2—asp 1
			aro 2—asp 2
	aro 3—ox time		resins—asp 1
			resins—asp 2
			saturates—ox time
F2—F3	aro 2—ox time		aro 2—asp 3
			aro 3—resins
			asp 3—ox time

An explanation of these correlations is provided in the following lines. First, aromatics 2 and 3 were the least polar fractions, which were anticorrelated with oxidation time, indicating a decrease in their contents. The aromatic 2 and 3 subfamilies could be considered the starting points of the aging process—the molecular classes most kinetically susceptible to change. In contrast, saturates and asphaltenes 3 were not correlated with oxidation time, meaning that they were not affected by the aging process. Only one anticorrelation between the active variables aromatics 2 and the resins was observed. This anticorrelation suggested the existence of a link between these two SAR-AD subfamilies during PAV aging, meaning a transformation of aromatics 2 into resins. As
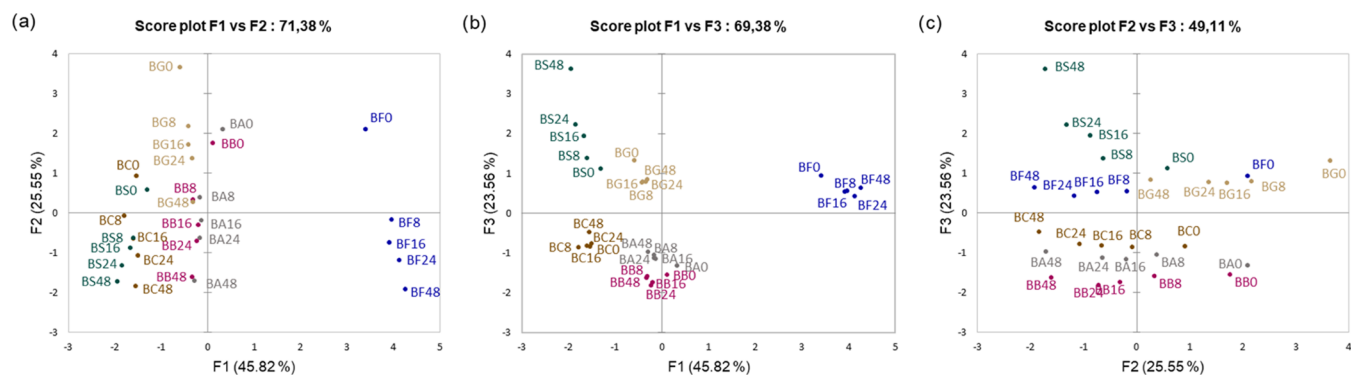
Figure 11. Score plots of 6 asphalts: (a) F1 vs F2, 71.4% explained variability; (b) F1 vs F3, 69.4% explained variability; (c) F2 vs F3, 49.1% explained variability.
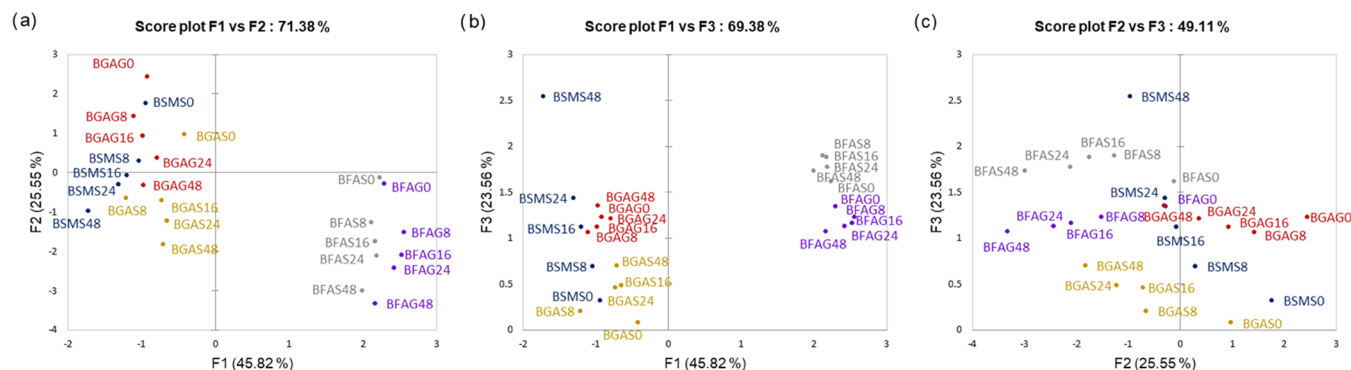

Figure 12. Score plots of the 5 asphalt blends used as additional observations: (a) F1 vs F2, 71.4% explained variability; (b) F1 vs F3, 69.4% explained variability; and (c) F2 vs F3, 49.1% explained variability.

Figure 13. Score plots of the 3 maltenes used as additional observations: (a) F1 vs F2, 71.4% explained variability; (b) F1 vs F3, 69.4% explained variability; and (c) F2 vs F3, 49.1% explained variability.
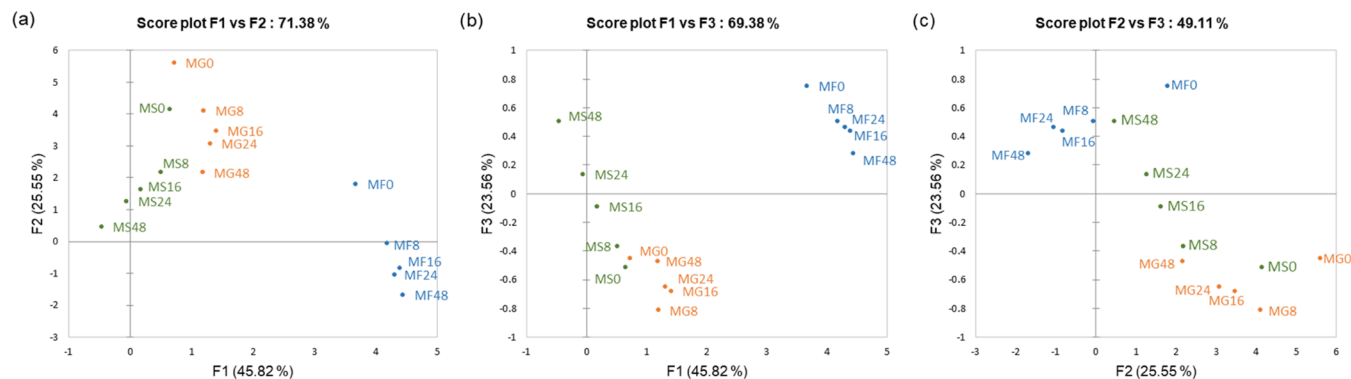
asphaltenes 1 and 2 were correlated, their content increased together during aging. The last type of observation addressed the lack of correlation between variables. Aromatics 2, aromatics 3, and resins presented several noncorrelations with other SAR-AD subfamilies. Aromatics 2 were not correlated with asphaltenes 1, 2, and 3, indicating that aromatics 2 were converted into resins and that the process seemed to stop at this stage. A lack of correlation between aromatics 3 and resins was observed, meaning that aromatics 3 were converted into asphaltenes. The conversion of aromatics 3 to asphaltenes was not correlated with any specific asphaltene subfamily type. The resins were not correlated with asphaltenes 1 and 2, meaning that they were not converted into those two subfamilies. However, for asphalt S,

the resin content decreased during aging, and conversion into asphaltenes 3 was observed.

The last part of the statistical study is the examination of the six asphalts in the 3 plans of the PCA. The 3 score plots combining PCs two by two presented in Figure 11 show the outcomes of this analysis. With the score plots F1 vs F2 (Figure 11a) and F1 vs F3 (Figure 11b), it was possible to confirm the significance of the F1 PC. By studying the repartition of the different asphalts along axis F1, it was possible to separate the 6 asphalts into 3 major classes. On the positive F1 values of approx. 4, there was asphalt F, which has the lowest asphaltene content from the sample series with 1.7 wt %. On the intermediate F1 value of approximately 0, it was possible to identify asphalts A, B, and G, which are

characterized by intermediate asphaltene contents of 6.6, 8.7, and 10.2 wt %, respectively. On the negative F1 values around −2, the last two asphalts C and S presented the highest asphaltene contents of 12.3 and 15.6 wt %, respectively. According to these observations, it was suggested that axis F1 was driven by the asphaltene content of the studied neat asphalts.

The second PC F2 is represented in Figure 11a (F1 vs F2) and Figure 11c (F2 vs F3). In those figures, it was observed that data for neat and aged samples from the same asphalt were classified according to their oxidation time on axis F2. The F2 values decreased when the oxidation time increased. It seemed that PC F2 was correlated with the PAV aging time, which is confirmed by the observations previously described with the correlation circles.

The significance of the third PC F3 is determined in Figure 11b,c. Figure 11b shows that data points representing neat and aged samples for 5 of the 6 asphalts (asphalts A, B, C, G, and F) were agglomerated. For these samples, the F3 values remained unchanged during PAV aging. However, data points corresponding to neat and aged asphalt S samples exhibited a different evolution. Asphalt S showed an increase in the F3 value according to the PAV aging time. By connecting this observation with the observations previously made in this paper that only asphalt S exhibited an increase in asphaltene 3 during PAV aging, an additional focus was placed on asphaltenes 3.

To confirm previous results, maltenes and asphalt blends were studied as additional observations to observe their behavior in the previously defined F1, F2, and F3 systems (Figures 12 and 13). Figures 12a−c and 13a−c could be used to confirm the significance of F2 PC. For each sample, F2 values decreased with increasing PAV aging time, confirming that F2 PC corresponded to a classification according to oxidation time and its impact on SAR-AD subfamilies during aging. By analyzing the evolution of asphalt blends presented in Figure 12b,c and that of maltenes presented in Figure 13b,c, it was possible to confirm the hypothesis made earlier for F3 significance. Among all studied samples added as additional variables, only 1 of the 5 asphalt blends and 1 of 3 of the maltenes displayed a particular behavior on the F3 axis; BSMS and MS, the two products made from asphalt S, showed this behavior. In contrast, for all other samples (BFAS, BFAG, BGAG, BGAS, MS, and MF), the amount of asphaltene 3 remained almost constant during PAV aging. As described previously, BSMS and MS presented the same increase in the asphaltene 3 amount as asphalt S during PAV aging, reinforcing that F3 PC corresponded to the evolution of the asphaltene 3 subfamily.

To summarize all of the findings from the first PCA and SAR-AD analysis, the following aging pathways could be proposed. For the six studied asphalts A, B, C, F, G, and S, it was identified that only aromatics 2 were converted into resins. For asphalts A, B, C, F, and G, no further conversion was observed, and the process stopped at this stage. However, for asphalt S, resins were converted into asphaltenes 3, but this creation of asphaltenes 3 was limited. For the six studied asphalts A, B, C, F, G, and S, it was identified that aromatics 3 were converted into asphaltenes 1 and/or 2. The PCA study did not identify that this pathway involved a transition through the resin subfamily with the samples used in the study. The saturate and aromatic 1 subfamilies were not affected or were minimally affected by the aging process.

Due to the particular chemical composition of asphalts F and S (asphaltene content), a second PCA was performed on the four remaining asphalts (A, B, C, and G) with similar origins to confirm or show new conversion pathways during aging. This second PCA was calculated with a database of 160 individuals (4 asphalts, 5 aging durations, and 8 subfamilies), and three PCs were once again considered to reach 95.7% cumulative variability. For this PCA, oxidation time was anticorrelated with PCs F3 and F1 (Table 6).

Table 6. Correlation Values between 8 Variables and the 3 Principal Components Calculated from Asphalts A, B, C, and G[a]

variables	F1	F2	F3
saturates	**0.762**	−0.323	−0.491
aro 1	0.138	0.605	**0.746**
aro 2	**0.979**	0.054	0.121
aro 3	0.388	−0.551	**0.730**
resins	**−0.800**	−0.515	−0.142
asp 1	**−0.950**	0.131	0.182
asp 2	**−0.873**	0.435	−0.143
asp 3	0.573	**0.726**	−0.342
oxidation time in PAV	−0.564	0.148	**−0.723**

[a]Bold values are values superior at |0.620| and considered significant.

The best representation of oxidation time appeared to be on the F1−F3 plan (Figure 14), with a correlation coefficient reaching 0.917. In this figure, the 8 SAR-AD variables were well represented on this plan with a significant correlation (|r| > 0.620).[45] The first principal component F1 once again seemed to express the asphaltenic character of the neat asphalt, with the most polar subfamilies on the left and the least on the
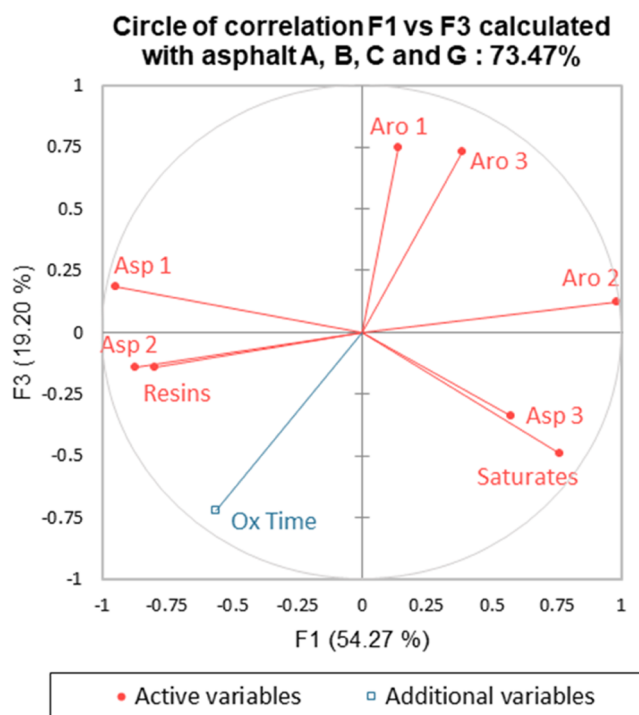

Figure 14. Circle of correlation calculated with the 4 asphalts A, B, C, and G: F1 vs F3: 73.5% of variability explained.

right. As previously performed with the first PCA, the outcomes of this second PCA are summarized in Table 7.

Table 7. Summary of Correlations between Variables Deduced from the F1−F3 Circle

plan	anticorrelation	correlation	no correlation
F1−F3	saturates−asp 1	saturates−asp 3	saturates−aro 3
	aro 2−resins		aro 1−asp 1
	aro 2−asp 2		aro 3−asp 3
	asp 1−asp 3	resins−asp 2	aro 3−asp 1
	aro 1−ox time		saturates−ox time
	aro 3−ox time		asp 3−ox time

In this second PCA, Table 7 confirms the observations and conclusions made with the first PCA regarding the two main asphalt aging pathways proposed above, namely, only aromatics 2 were converted into resins and aromatics 3 were converted into asphaltenes 1 and/or 2. The second PCA also generated additional insights into the behavior of the subfamily conversions during oxidation, and the aromatics 1 were anticorrelated with the oxidation time but did not exhibit any anticorrelations with SAR-AD active variables. This observation suggested a conversion of aromatics 1 into different more polar SAR-AD subfamilies, but no specific pathway could be identified.

In addition, asphaltenes 3 were not correlated with the oxidation time, which confirmed that this SAR-AD subfamily (even if it is the more polar one constituting the asphalt) did not play a key role in the aging process. This also confirmed that asphalt S presented a particular behavior during PAV aging with an extra aging pathway not observed with the other asphalts. Investigation of asphalt S chemistry using mass spectrometry and/or elementary analysis for each subfamily could be useful to explain the creation of asphaltenes 3. For example, this phenomenon could be hypothetically due to a higher content of sulfur in some SAR-AD subfamilies of asphalt S.

CONCLUSIONS

This study, which sought to assess if the SAR-AD technology could help to better understand asphalt PAV aging impact on asphalt chemistry, provided interesting and innovative learnings. Several asphalts, maltenes, and asphalt blends were selected for their difference in chemical composition. They were aged with the PAV method and analyzed with the SAR-AD. This chromatographic technology combined with principal component analysis is an innovative approach allowing the observation of new aging pathways vs those generally observed using SARA data. From the correlations, anticorrelations, and no correlations given by the PCA, two aging pathways were proposed with aromatics 2 and 3 as starting points.

(1) The first aging pathway was the conversion of aromatics 2 into resins without further creation of asphaltenes for five of the six tested asphalts. Only one asphalt (S) showed a conversion of the resins into asphaltenes 3.

(2) The second one was the conversion of aromatics 3 (the most abundant and polar aromatic subfamily) directly into asphaltenes 1 and/or 2.

(3) Saturates and aromatics 1 (sometimes described as naphtheno-aromatics) were the least affected by the aging process.

To conclude, this study suggested that the conversion of SAR-AD subfamilies during PAV aging was not necessarily to the closest subfamily in terms of polarity. Consequently, asphaltene molecules could be created without involving resins.

ASSOCIATED CONTENT

Ⓢ Supporting Information

The Supporting Information is available free of charge at https://pubs.acs.org/doi/10.1021/acsomega.2c07754.

SAR-AD subfamilies quantification before and after PAV aging (PDF)

AUTHOR INFORMATION

Corresponding Authors

Séverine Tisse − *Univ Rouen Normandie, FR3038, SMS, UR 3233, F-76000 Rouen, France;* ⓞ orcid.org/0000-0003-2050-257X; Email: severine.tisse@univ-rouen.fr

Laurent Michon − *Esso SAF, F-76330 Port-Jérôme-sur-Seine, France;* Email: laurent.michon@exxonmobil.com

Authors

Lorris Bruneau − *Esso SAF, F-76330 Port-Jérôme-sur-Seine, France; Univ Rouen Normandie, FR3038, SMS, UR 3233, F-76000 Rouen, France*

Pascal Cardinael − *Univ Rouen Normandie, FR3038, SMS, UR 3233, F-76000 Rouen, France;* ⓞ orcid.org/0000-0001-8828-4527

Complete contact information is available at:
https://pubs.acs.org/10.1021/acsomega.2c07754

Notes

The authors declare no competing financial interest.

REFERENCES

(1) Branthaver, J. F.; Harnsberger, P. M.; Mill, T.; Ensley, E. K.; Barbour, F. A.; Schabron, J. F.Binder Characterization and Evaluation Volume 2: Chemistry *Strateg. Highw. Res. Program* 1993, pp 1−527.

(2) Petersen, J. C. A Review of the Fundamentals of Asphalt Oxidation Chemical, Physicochemical, Physical Property, and Durability Relationships, E-C140 *Transp. Res. Rec.*, 2009.

(3) Wang, F.; Xiao, Y.; Cui, P.; Lin, J.; Li, M.; Chen, Z. Correlation of Asphalt Performance Indicators and Aging Degrees: A Review. *Constr. Build. Mater.* **2020**, *250*, No. 118824.

(4) Qin, Q.; Schabron, J. F.; Boysen, R. B.; Farrar, M. J. Field Aging Effect on Chemistry and Rheology of Asphalt Binders and Rheological Predictions for Field Aging. *Fuel* **2014**, *121*, 86−94.

(5) Afnor. Bitumen and Bituminous Binders — Accelerated Long-Term Ageing Conditioning by a Pressure Ageing Vessel (PAV); EN 14769, 2012.

(6) Lienemann, C. P. Analyse de métaux traces dans les produits pétroliers, état de l'art. *Oil Gas Sci. Technol.* **2005**, *60*, 951−965.

(7) Traxler, R. N.; Scrivner, F. H.Loss of Durability in Bituminous Pavement Surfaces--Importance of Chemically Active Solar Radiation *Tex. Transp. Inst.* 1971, pp 1–74.

(8) Branthaver, J. F.; Nazir, M.; Petersen, J. C.; Dorrence, S. M. The Effect of Metalloporphyrins on Asphalt Oxidation. I. Effect of Synthetic Metal Chelates. *Liq. Fuels Technol.* 1983, *1*, 355–369.

(9) Lacroix-Andrivet, O.; Maillard, J.; Siqueira, A. L. M.; Hubert-Roux, M.; Loutelier-Bourhis, C.; Afonso, C. Molecular Characterization of Aged Bitumen with Selective and Nonselective Ionization Methods by Fourier Transform Ion Cyclotron Resonance Mass Spectrometry. 2. Statistical Approach on Multiple-Origin Samples. *Energy Fuels* 2021, *35*, 16442–16451.

(10) Neumann, A.; Käfer, U.; Gröger, T.; Wilharm, T.; Zimmermann, R.; Rüger, C. P. Investigation of Aging Processes in Bitumen at the Molecular Level with High-Resolution Fourier-Transform Ion Cyclotron Mass Spectrometry and Two-Dimensional Gas Chromatography Mass Spectrometry. *Energy Fuels* 2020, *34*, 10641–10654.

(11) Zhang, M.; Hao, P.; Dong, S.; Li, Y.; Yuan, G. Asphalt Binder Micro-Characterization and Testing Approaches: A Review. *Measurement* 2020, *151*, No. 107255.

(12) Feng, Z.-g.; Wang, S.-j.; Bian, H.-j.; Guo, Q.-l.; Li, X.-j. FTIR and Rheology Analysis of Aging on Different Ultraviolet Absorber Modified Bitumens. *Constr. Build. Mater.* 2016, *115*, 48–53.

(13) Cong, P.; Liu, N.; Tian, Y.; Zhang, Y. Effects of Long-Term Aging on the Properties of Asphalt Binder Containing Diatoms. *Constr. Build. Mater.* 2016, *123*, 534–540.

(14) Mouillet, V.; Lamontagne, J.; Durrieu, F.; Planche, J.-P.; Lapalu, L. Infrared Microscopy Investigation of Oxidation and Phase Evolution in Bitumen Modified with Polymers. *Fuel* 2008, *87*, 1270–1280.

(15) Hofko, B.; Porot, L.; Falchetto Cannone, A.; Poulikakos, L.; Huber, L.; Lu, X.; Mollenhauer, K.; Grothe, H. FTIR Spectral Analysis of Bituminous Binders: Reproducibility and Impact of Ageing Temperature. *Mater. Struct.* 2018, *51*, No. 45.

(16) Soenen, H.; Lu, X.; Laukkanen, O.-V. Oxidation of Bitumen: Molecular Characterization and Influence on Rheological Properties. *Rheol. Acta* 2016, *55*, 315–326.

(17) Jiang, W.; Bao, R.; Lu, H.; Yuan, D.; Lu, R.; Sha, A.; Shan, J. Analysis of Rheological Properties and Aging Mechanism of Bitumen after Short-Term and Long-Term Aging. *Constr. Build. Mater.* 2021, *273*, No. 121777.

(18) Themeli, A.; Chailleux, E.; Farcas, F.; Chazallon, C.; Migault, B.; Buisson, N. Molecular Structure Evolution of Asphaltite-Modified Bitumens during Ageing; Comparisons with Equivalent Petroleum Bitumens. *Int. J. Pavement Res. Technol.* 2017, *10*, 75–83.

(19) Yang, C.; Xie, J.; Wu, S.; Amirkhanian, S.; Zhou, X.; Ye, Q.; Yang, D.; Hu, R. Investigation of Physicochemical and Rheological Properties of SARA Components Separated from Bitumen. *Constr. Build. Mater.* 2020, *235*, No. 117437.

(20) Cannone Falchetto, A.; Alisov, A.; Goeke, M.; Wistuba, M. P. In *Identification of Structural Changes in Bitumen Due to Aging and Fatigue*, Proceedings of 6th Eurasphalt & Eurobitume Congress; Czech Technical University: Prague, 2016.

(21) Corbett, L. W. Composition of Asphalt Based on Generic Fractionation, Using Solvent Deasphaltening, Elution-Adsorption Chromatography, and Densimetric Characterization. *Anal. Chem.* 1969, *41*, 576–579.

(22) Western Research Institute. *Automated High-Performance Liquid Chromatography Saturate, Aromatic, Resin, and Asphaltene Separation*; Federal Highway Administration, 2016.

(23) Fallah, F.; Khabaz, F.; Kim, Y.-R.; Kommidi, S. R.; Haghshenas, H. F. Molecular Dynamics Modeling and Simulation of Bituminous Binder Chemical Aging Due to Variation of Oxidation Level and Saturate-Aromatic-Resin-Asphaltene Fraction. *Fuel* 2019, *237*, 71–80.

(24) Hu, Y.; Si, W.; Kang, X.; Xue, Y.; Wang, H.; Parry, T.; Airey, G. D. State of the Art: Multiscale Evaluation of Bitumen Ageing Behaviour. *Fuel* 2022, *326*, No. 125045.

(25) Mirwald, J.; Werkovits, S.; Camargo, I.; Maschauer, D.; Hofko, B.; Grothe, H. Investigating Bitumen Long-Term-Ageing in the Laboratory by Spectroscopic Analysis of the SARA Fractions. *Constr. Build. Mater.* 2020, *258*, No. 119577.

(26) Mirwald, J.; Werkovits, S.; Camargo, I.; Maschauer, D.; Hofko, B.; Grothe, H. Understanding Bitumen Ageing by Investigation of Its Polarity Fractions. *Constr. Build. Mater.* 2020, *250*, No. 118809.

(27) Hung, A. M.; Fini, E. H. Absorption Spectroscopy to Determine the Extent and Mechanisms of Aging in Bitumen and Asphaltenes. *Fuel* 2019, *242*, 408–415.

(28) Wang, K.; Yuan, Y.; Han, S.; Yang, H. Application of Attenuated Total Reflectance Fourier Transform Infrared (ATR-FTIR) and Principal Component Analysis (PCA) for Quick Identifying of the Bitumen Produced by Different Manufacturers. *Road Mater. Pavement Des.* 2018, *19*, 1940–1949.

(29) Ren, R.; Han, K.; Zhao, P.; Shi, J.; Zhao, L.; Gao, D.; Zhang, Z.; Yang, Z. Identification of Asphalt Fingerprints Based on ATR-FTIR Spectroscopy and Principal Component-Linear Discriminant Analysis. *Constr. Build. Mater.* 2019, *198*, 662–668.

(30) Margaritis, A.; Soenen, H.; Fransen, E.; Pipintakos, G.; Jacobs, G.; Blom, J.; Van den bergh, W. Identification of Ageing State Clusters of Reclaimed Asphalt Binders Using Principal Component Analysis (PCA) and Hierarchical Cluster Analysis (HCA) Based on Chemo-Rheological Parameters. *Constr. Build. Mater.* 2020, *244*, No. 118276.

(31) Afnor. Bitumen and Bituminous Binders — Specifications for Paving Grade Bitumens; EN 12591, 2015.

(32) D04 Committee. *Test Method for Separation of Asphalt into Four Fractions*: ASTM International.

(33) Mousavi, M.; Abdollahi, T.; Pahlavan, F.; Fini, E. H. The Influence of Asphaltene-Resin Molecular Interactions on the Colloidal Stability of Crude Oil. *Fuel* 2016, *183*, 262–271.

(34) Mousavi, M.; Pahlavan, F.; Oldham, D.; Abdollahi, T.; Fini, E. H. Alteration of Intermolecular Interactions between Units of Asphaltene Dimers Exposed to an Amide-Enriched Modifier. *RSC Adv.* 2016, *6*, 53477–53492.

(35) Omairey, E. L.; Zhang, Y.; Al-Malaika, S.; Sheena, H.; Gu, F. Impact of Anti-Ageing Compounds on Oxidation Ageing Kinetics of Bitumen by Infrared Spectroscopy Analysis. *Constr. Build. Mater.* 2019, *223*, 755–764.

(36) Arndt, J. H.; Macko, T.; Brüll, R. Application of the Evaporative Light Scattering Detector to Analytical Problems in Polymer Science. *J. Chromatogr. A* 2013, *1310*, 1–14.

(37) Pahlavan, F.; Hosseinnezhad, S.; Samieadel, A.; Hung, A.; Fini, E. Fused Aromatics To Restore Molecular Packing of Aged Bituminous Materials. *Ind. Eng. Chem. Res.* 2019, *58*, 11939–11953.

(38) Mousavi, M.; Pahlavan, F.; Oldham, D.; Hosseinnezhad, S.; Fini, E. H. Multiscale Investigation of Oxidative Aging in Biomodified Asphalt Binder. *J. Phys. Chem. C* 2016, *120*, 17224–17233.

(39) Adams, J.; Rovani, J.; Boysen, R. B.; Elwardany, M. D.; Planche, J.-P. Innovations and Developments in Bitumen Composition Analysis, 2021.

(40) Lesueur, D. The Colloidal Structure of Bitumen: Consequences on the Rheology and on the Mechanisms of Bitumen Modification. *Adv. Colloid Interface Sci.* 2009, *145*, 42–82.

(41) D'Melo, D.; Gupta, R.; Bhattacharya, S.; Taylor, R.; Holkar, C. Impact of Asphaltene Chemistry on Bitumen Properties, 2021.

(42) Redelius, P. Asphaltenes in Bitumen, What They Are and What They Are Not. *Road Mater. Pavement Des.* 2009, *10*, 25–43.

(43) Powers, D. P.; Sadeghi, H.; Yarranton, H. W.; van den Berg, F. G. A. Regular Solution Based Approach to Modeling Asphaltene Precipitation from Native and Reacted Oils: Part 1, Molecular Weight, Density, and Solubility Parameter Distributions of Asphaltenes. *Fuel* 2016, *178*, 218–233.

(44) Dereppe, J.-M.; Moreaux, C.; Castex, H. Analysis of Asphaltenes by Carbon and Proton Nuclear Magnetic Resonance Spectroscopy. *Fuel* 1978, *57*, 435–441.

(45) Anderson, T. W. *An Introduction to Multivariate Statistical Analysis*; Wiley: New York, 1984.